

A Newton-Galerkin method for fluid flow exhibiting uncertain periodic dynamics

M. Schick^{‡*}, V. Heuveline[§], and O. P. Le Maître^{¶†}

Abstract. The determination of stable limit-cycles plays an important role for quantifying the characteristics of dynamical systems. In practice exact knowledge of model parameters is rarely available leading to parameter uncertainties, which can be modeled as an input of random variables. This has the effect that the limit-cycles become stochastic themselves resulting in almost surely time-periodic solutions with a stochastic period. In this paper we introduce a novel numerical method for the computation of stable stochastic limit-cycles based on the Spectral-Stochastic-Finite-Element-Method using Polynomial Chaos (PC). We are able to overcome the difficulties of Polynomial Chaos regarding its well known convergence breakdown for long term integration. To this end, we introduce a stochastic time scaling which treats the stochastic period as an additional random variable and controls the *phase-drift* of the stochastic trajectories, keeping the necessary PC order low. Based on the re-scaled governing equations, we aim at determining an initial condition and a period such that the trajectories close after completion of one stochastic cycle. Furthermore, we verify the numerical method by computation of a vortex shedding of a flow around a circular domain with stochastic inflow boundary conditions as a benchmark problem. The results are verified by comparison to purely deterministic reference problems and demonstrate high accuracy up to machine precision in capturing the stochastic variations of the limit-cycle.

Key words. uncertainty quantification, stochastic limit-cycle, stochastic Navier-Stokes equations, stochastic period, polynomial chaos, long term integration

AMS subject classifications. 35K55, 37N10, 65C20, 65M60, 65M70

1. Introduction. Many fluid flows can be modeled by the unsteady incompressible Navier-Stokes equations, solutions of which can exhibit different dynamics. Among these dynamics stable limit-cycles play an important role, for example in the study of flow transition from laminar to turbulent regimes or limit-cycle-oscillations in flow-induced vibration analysis. In the deterministic context, there exist various numerical methods to determine limit-cycles, see for example [3, 4]. However, in practice, flow parameters like the kinematic viscosity, external forcing or boundary conditions are subjected to uncertainties, either arising from a lack of knowledge (epistemic type) or intrinsic variability (aleatoric type). For sensitivity analysis, the uncertainties can be modeled by vectors of independent random variables and propagated within the solution. This, however, leads to a significant increase in computational complexity

*Corresponding author. Email: Michael.Schick@h-its.org

†The work of OLM is supported in part by the French Agence Nationale pour la Recherche (Project ANR-2010-Blan-0904), by the US Department of Energy, Office of Advanced Scientific Computing Research, Award Number DE-SC0007020, and the SRI Center for Uncertainty Quantification at the King Abdullah University of Science and Technology

‡Engineering Mathematics and Computing Lab (EMCL), Karlsruhe Institute of Technology (KIT), 76133 Karlsruhe, Germany. New address: Heidelberg Institute for Theoretical Studies, 69118 Heidelberg, Germany

§Engineering Mathematics and Computing Lab (EMCL), Karlsruhe Institute of Technology (KIT), 76133 Karlsruhe, Germany. New address: Interdisciplinary Center for Scientific Computing, Heidelberg University, 69115 Heidelberg, Germany

¶LIMSI-CNRS, 91403 Orsay cedex, France; Department of Mechanical Engineering and Materials Science, Duke University, Durham, NC 27708

compared to purely deterministic models and requires efficient algorithms.

In presence of random inputs, the limit-cycles generally become random quantities, and if the solution is almost surely time-periodic the stochastic limit-cycle can be characterized by a (non-unique) stochastic initial condition and a stochastic period. Assuming a second order solution, spectral methods provide a powerful tool to represent smooth dependencies of the limit-cycle on the random input. For instance, the Karhunen-Loève expansion is optimal in mean-square sense with a truncation error governed by the decay rate of the covariance operator's eigenvalues. Polynomial Chaos (PC) expansions, based on the seminal works of Wiener [29] and Ghanem and Spanos [8], aim at expressing the solution as a series of predefined random functionals without prior information on the structure of the solution. The PC basis functionals are orthogonal multivariate polynomials in the random input variables whose probability law is defined *a priori*. Therefore, the coefficients within the expansion need to be determined. One popular approach is given by non-intrusive methods, such as Monte Carlo or sparse-grid methods, which have the benefit to allow for embarrassingly parallel computational strategies. An alternative approach, which is used within this work, is given by stochastic Galerkin projections, where the governing equations are projected on the space spanned by the Polynomial Chaos basis. Thereby, one fully coupled system has to be solved allowing to compute the PC coefficients at once at the price of a significantly increased system size.

However, it is known that PC expansions can exhibit a convergence breakdown in cases of strong non-linear dynamics and for long term integration [18]. This is related to the fact that trajectories corresponding to random input realizations exhibit a *phase-drift*, which requires a growing polynomial degree of the PC expansion to accurately capture the non-linear dependencies in time. In [28] a multi-element approach was introduced, which is able to postpone the point of convergence breakdown to later simulation times based on a domain decomposition of the probability space. In [2] a similar idea was developed employing a wavelet multi-resolution analysis [15, 19], which, however, also suffers from the same drawback regarding the long term integration convergence breakdown. Recently, a time-dependent basis for capturing the time evolution of the probability distribution of the solution was introduced in [7, 24]. In [10] an extension to [7] was proposed, which combines time-dependent basis functionals with the domain decomposition introduced in [28] to improve numerical stability.

All these methods allow to compute stable limit-cycles by means of classical time-integration, owing to an enrichment of the stochastic basis or a costly time-adaption of the basis functionals. In fact, none of these approaches addresses the central difficulty which is related to *phase-drift* between realizations. Our claim is that, in many situations, random phase information has no relevance and can be set arbitrarily, while only the dependencies of the limit-cycle is of interest. In such cases, the random limit-cycle can be simply defined using an arbitrary random initial condition belonging to the limit-cycle and the random period. The potential advantage for this description of the dynamics lies in the fact that the random solution at any phase can be subsequently recovered by time-integration from the initial condition over *at most* one period, so avoiding the need of particular treatment required for long term integration. The principal focus of the present work is to demonstrate the validity of this description and to verify that it allows for low degree PC expansions. To the present knowledge of the authors, there do not exist numerical algorithms to compute stochastic limit-

cycles with uncertain period using Polynomial Chaos expansions. Overcoming the drawback of the convergence breakdown of PC, we introduce a new numerical algorithm, which is able to determine stochastic limit-cycles subject to a stochastic period, based on a stochastic time rescaling of the unsteady incompressible Navier-Stokes equations, Newton's method and an optimality constraint. In addition, inspired by the ideas proposed in [18] we introduce a secondary stochastic time scaling to control the *phase-drift* in an L^2 -sense with respect to some deterministic reference trajectory. The numerical solution of the stochastic systems is obtained using the Spectral-Stochastic-Finite-Element-Method (SSFEM), which is based on a Galerkin projection of the governing equations on the probability space spanned by the Chaos Polynomials combined with a Finite-Element discretization at the deterministic level. We finally verify the convergence properties of the algorithm for two-dimensional flows around a circular domain with stochastic inflow boundary conditions. The problem configuration yields a time-periodic vortex shedding, known as Kàrmàn vortex street, which depends on the inflow conditions.

The paper is structured as follows. Section 2 introduces the unsteady stochastic incompressible Navier-Stokes equations along with the problem definition of finding almost surely time-periodic solutions. Section 3 describes the numerical method to compute an initial condition and the period of the random flow, together with the control of the *phase-drift*. The convergence properties of the algorithm are verified using adequate benchmark problems in Section 4. Finally, Section 5 provides a short summary and conclusions of this work.

2. Model equations and problem definition.

2.1. Unsteady stochastic incompressible Navier-Stokes equations. It is assumed that there exists a stochastic model, which appropriately describes the underlying uncertainties within the considered system. Furthermore, it is assumed that the uncertainties can be parametrized via some random vector $\xi = (\xi_1, \dots, \xi_L) \in \mathbb{R}^L$ of dimension $L \in \mathbb{N}$, where $\xi_i, i = 1, \dots, L$, are independent real-valued random variables and ξ belongs to some underlying probability space $(\Omega, \mathcal{F}, \mathbb{P})$. The uncertainties shall be introduced via boundary or initial conditions. The parametrized unsteady stochastic incompressible Navier-Stokes equations (SNSE) read:

$$\partial_t u(x, t, \xi) + (u(x, t, \xi) \cdot \nabla)u(x, t, \xi) - \nu \Delta u(x, t, \xi) + \nabla p(x, t, \xi) = 0, \quad \text{in } \mathcal{D}, \quad (2.1)$$

$$\nabla \cdot u(x, t, \xi) = 0, \quad \text{in } \mathcal{D}, \quad (2.2)$$

$$u(x, t, \xi) = g(x, t, \xi), \quad \text{on } \Gamma, \quad (2.3)$$

$$u(x, t = 0; \xi) = u_I(x, \xi), \quad \text{in } \mathcal{D}, \quad (2.4)$$

for $t > 0$ almost surely in Ω . Here, $\mathcal{D} \subset \mathbb{R}^d$, $d = 2, 3$ denotes the spatial domain with Dirichlet boundary $\Gamma \subset \partial \mathcal{D}$.

Note that $u = u(x, t; \xi)$ is a random field due to the explicit dependency on the random vector ξ through the partial differential equation. The SNSE can be solved relying on Polynomial Chaos (PC) expansions of the velocity and pressure fields and using the stochastic Galerkin projection method (see e.g. [13, 14, 16] and references in [17]). However, if the SNSE possess no stable steady solution a high order PC expansion is expected to be necessary for long term integration, even if the individual realizations exhibit almost surely asymptotically

periodic dynamics. This fact motivates the direct determination of the stochastic periodic solutions instead of proceeding from straightforward time-integration of the PC system.

2.2. Periodic orbits. We introduce a new numerical method for determining solutions of the SNSE, which are almost surely periodic subject to a stochastic period, by extending a deterministic approach introduced by Duguet et al. [4] using the Spectral-Stochastic-Finite-Element-Method [8]. This makes it possible to characterize all trajectories of the random events by a functional representation of the stochastic period and an initial condition with respect to the random input by using a Polynomial Chaos expansion.

For the remainder of this work we provide abbreviated definitions of repeatedly occurring vector spaces for notational convenience:

$$\mathcal{S} := L^2(\Omega), \quad V := H^1(\mathcal{D}), \quad V_0 := H_0^1(\mathcal{D}), \quad W := L^2(\mathcal{D}).$$

A fundamental assumption about existence of a time-periodic solution needs to hold:

Assumption 1. *There exists a solution u to (2.1)–(2.4), $u(\cdot, t, \cdot) \in V \otimes \mathcal{S}$, $t \geq 0$, and a bounded period $T \in \mathcal{S}$ with $\alpha \leq T < \infty$ a.s. for some $\alpha > 0$, such that for $t \geq 0$:*

$$u(x, t + T(\xi); \xi) = u(x, t; \xi), \quad \forall x \in \overline{\mathcal{D}}, \quad a.s.$$

The main problem in computing stochastic periodic orbits arises from the stochastic nature of the period T . A discretization based on a deterministic time stepping method will have difficulties in capturing the stochastic variations of the period, since the trajectories of a solution to the SNSE depend on a random event $\omega \in \Omega$. The approach outlined in the following aims at representing the stochastic period as some additional random input within the SNSE, introducing a new random variable, whose computation introduces an additional condition. This allows the use of a deterministic simulation time interval to compute an initial condition and a period, since the uncertainty within the time interval is transferred towards the system equations.

We introduce a new scaled time variable λ which is defined for $t \geq 0$ by:

$$\lambda(t, \xi) := \frac{t}{T(\xi)}, \quad \text{pointwise in } \Omega. \quad (2.5)$$

Note that λ is a random process and $\lambda(t, \cdot) \in \mathcal{S}$ for $t \geq 0$ provided that the period T satisfies Assumption 1. Introducing the scaled time λ into (2.1)–(2.3) results in a scaled version of the unsteady stochastic incompressible Navier-Stokes equations (S-SNSE) for $\lambda > 0$:

$$\begin{aligned} \partial_\lambda \tilde{u}(x, \lambda, \xi) + T(\xi)(\tilde{u}(x, \lambda, \xi) \cdot \nabla) \tilde{u}(x, \lambda, \xi) \\ - \nu T(\xi) \Delta \tilde{u}(x, \lambda, \xi) + \nabla \tilde{p}(x, \lambda, \xi) = 0, \end{aligned} \quad \text{in } \mathcal{D}, \quad (2.6)$$

$$\nabla \cdot \tilde{u}(x, \lambda, \xi) = 0, \quad \text{in } \mathcal{D}, \quad (2.7)$$

$$\tilde{u}(x, \lambda, \xi) = g(x, \lambda, \xi), \quad \text{on } \Gamma, \quad (2.8)$$

$$\tilde{u}(x, \lambda = 0, \xi) = u_I(x, \xi), \quad \text{in } \mathcal{D}, \quad (2.9)$$

almost surely in Ω . Note that the velocity and pressure variables have been redefined by:

$$\tilde{u}(x, t/T(\xi), \xi) := u(x, t, \xi), \quad \tilde{p}(x, t/T(\xi), \xi) := T(\xi)p(x, t, \xi). \quad (2.10)$$

In the following the tilde notation will be dropped for notational convenience.

2.3. Discretization and variational formulation. The discretization of the probability space is carried out by a Galerkin projection employing Polynomial Chaos.

First, velocity and pressure fields u, p are approximated by their corresponding Polynomial Chaos expansion employing a finite truncation parameter P :

$$[u(x, \lambda; \xi), p(x, \lambda; \xi)] = \sum_{i=0}^P [u_i(x, \lambda), p_i(x, \lambda)] \psi_i(\xi).$$

Here, the truncation parameter P satisfies $(P + 1) = (p + L)!/p!L!$, where $p \in \mathbb{N}$ is the maximum total polynomial degree of the normalized Chaos Polynomials ψ_i , $i = 0, 1, 2, \dots$. For notational convenience, we shall denote \mathcal{S}^P the subspace of \mathcal{S} spanned by the PC basis.

Next, the PC discretizations are inserted into the scaled Navier-Stokes equations (2.6)–(2.9) which are then projected onto \mathcal{S}^P , resulting in:

$$\begin{aligned} \partial_\lambda u_k(x, \lambda) + \sum_{j=0}^P \sum_{l=0}^P (u_j(x, \lambda) \cdot \nabla) u_l(x, \lambda) c(T)_{jlk} \\ - \sum_{j=0}^P \Delta u_j(x, \lambda) \nu(T)_{jk} + \nabla p_k(x, \lambda) = 0, \quad \text{in } \mathcal{D}, \end{aligned} \quad (2.11)$$

$$\nabla \cdot u_k(x, \lambda) = 0, \quad \text{in } \mathcal{D}, \quad (2.12)$$

$$u_k(x, \lambda) = \langle g, \psi_k \rangle, \quad \text{on } \Gamma, \quad (2.13)$$

$$u_k(x, \lambda = 0) = \langle u_I, \psi_k \rangle, \quad \text{in } \mathcal{D}, \quad (2.14)$$

for $\lambda > 0$ and $k = 0, \dots, P$. The angle brackets $\langle \cdot, \cdot \rangle$ denote the inner-product on \mathcal{S} and the 3rd and 2nd order tensors are defined by:

$$c(T)_{jlk} := \sum_{i=0}^Q T_i \langle \psi_i \psi_j \psi_l, \psi_k \rangle, \quad \nu(T)_{jk} := \nu \sum_{i=0}^Q T_i \langle \psi_i \psi_j, \psi_k \rangle.$$

for $j, l, k = 0, \dots, P$. For the period T , we again rely on a PC expansion, truncated to a maximum total polynomial degree q , so that

$$T(\xi) = \sum_{i=0}^Q T_i \psi_i(\xi), \quad Q + 1 = \frac{(q + L)!}{q!L!}.$$

We denote consistently \mathcal{S}^Q the corresponding subspace of \mathcal{S} .

Note that both tensors have many zero valued entries, especially when eventually a low order expansion for T will be employed. This significantly reduces the number of coupling terms in (2.11). Furthermore, the redefinition of the pressure variable in (2.10) plays an important role, since the pressure term appears completely decoupled in (2.11), which would not be the case if the pressure term would still involve a product with the stochastic period $T(\xi)$, as being the case for the viscosity term. However, the number of coupling terms within

(2.11) is significantly increased in comparison to a Galerkin projection of the standard unscaled formulation (2.1) due to the non-linear convective term.

A variational formulation (at the deterministic level) of the stochastic Galerkin system (2.11)–(2.14) is:

For $k = 0, \dots, P$, $\lambda > 0$ and given period modes T_k , find $u_k(\cdot, \lambda) \in V$ and $p_k(\cdot, \lambda) \in W$ such that $\forall v \in V_0, \forall q \in W$:

$$(\partial_\lambda u_k, v) + \sum_{j,l=0}^P ((u_j \cdot \nabla) u_l, v) c(T)_{jlk} + \sum_{j=0}^P (\nabla u_j, \nabla v) \nu(T)_{jk} - (p_k, \nabla \cdot v) = 0, \quad (2.15)$$

$$(\nabla \cdot u_k, q) = 0, \quad (2.16)$$

$$u_k(x, \lambda) = \langle g, \psi_k \rangle, \quad \text{on } \Gamma, \quad (2.17)$$

$$u_k(x, \lambda = 0) = \langle u_I, \psi_k \rangle, \quad \text{in } \mathcal{D}. \quad (2.18)$$

Here, (\cdot, \cdot) denotes the inner-product on W . We solve the coupled system (2.15)–(2.18) by means of a classical Finite-Element Method with finite dimensional spaces $V^h \subset V$ and $W^h \subset W$. For an overview on existing Finite-Element solvers for the deterministic Navier-Stokes equations see e.g. [6, 9, 27]. For solving and preconditioning (2.15)–(2.18) see e.g. [13, 14, 16, 20, 21].

2.4. Determining the period and initial condition. We define the following operator to track the velocity as a function of the scaled time variable $\lambda \geq 0$ subject to some period T and initial condition u_I :

$$\mathcal{U}(u_I, T, \lambda) := u_I + \int_0^\lambda \partial_\lambda u(\lambda = \sigma) d\sigma, \quad (2.19)$$

where u satisfies (2.15)–(2.18). Note, that \mathcal{U} represents the velocity at time λ starting from the initial condition u_I , whose PC expansion will be denoted by

$$\mathcal{U}(u_I, T, \lambda) = \sum_{i=0}^P \mathcal{U}_i(u_I, T, \lambda) \psi_i, \quad (2.20)$$

where $\mathcal{U}_i \in V$ for $i = 0, \dots, P$, such that $\mathcal{U}_i = \mathcal{U}_i(u_I, T, \lambda)(x) = u_i(x, \lambda)$ with u_i denoting the i^{th} mode of the PC expansion of the velocity u satisfying (2.15)–(2.18) at time λ .

The problem definition of finding almost surely time-periodic solutions to the S-SNSE can be formulated in the following way:

Find some u_I , whose PC coefficients satisfy (2.16)–(2.17), and a corresponding T as in Assumption 1, such that

$$\|\mathcal{U}(u_I, T, 1) - u_I\|^2 = 0, \quad (2.21)$$

where here and for the rest of this work $\|\cdot\| := \|\cdot\|_{\mathcal{S} \otimes W}$. Because of the truncation error, eq. (2.21) can only be formally satisfied if $u_I \in \mathcal{S}^P \otimes V$; otherwise a weak interpretation can be invoked. Note that the determination of the period T imposes an additional constraint on the S-SNSE. Therefore, we suggest an iterative approach, which will be explained in detail within the following section.

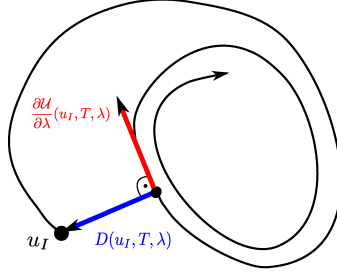


Figure 3.1: Schematic view of a trajectory starting at some initial condition u_I with distance vector D and time derivative $\frac{\partial \mathcal{U}}{\partial \lambda}$ for some realization of ξ .

3. Solution procedure. In the following an iterative method, inspired by an approach for deterministic problems introduced by Duguet et al. [4], will be described to compute an initial condition u_I and a period T satisfying (2.21), employing Newton's method, the solution of an optimization problem and an optimality based *phase-controlling*. The initial condition is sought in $\mathcal{S}^P \otimes V$, while a stochastic discretization of the period is needed.

For $\lambda \geq 0$ and some initial condition u_I we define a distance vector D by:

$$D(u_I, T, \lambda) := u_I - \mathcal{U}(u_I, T, \lambda),$$

Therefore, $\|D\|$ measures the distance between an initial condition u_I and its state $\mathcal{U}(u_I, T, \lambda)$ at time λ . The goal of the iteration procedure is to obtain convergence such that:

$$\|D(u_I^k, T^k, \lambda)\| \rightarrow 0 \quad \text{as } k \rightarrow \infty.$$

We start by choosing some appropriate initial guesses $u_I^0 = \sum_{i=0}^P u_{I,i}^0 \psi_i$ and $T^0 = \sum_{i=0}^Q T_i^0 \psi_i$ for the initial condition and period, respectively. As an initial guess for u_I^0 and corresponding T^0 we suggest to use a fully developed deterministic flow, i.e. $u_{I,i}^0 = 0$ and $T_i^0 = 0$ for $i > 0$, which has been computed *a priori* by integration of the deterministic Navier-Stokes equations parametrized by the mean of the random input.

3.1. An optimality constraint for determining the period. To arrive at an update formula for the period, we first define an optimization problem, which ensures that the distance between the initial condition and its terminal state remains minimal in a L^2 sense. Therefore, given the k th iterates u_I^k and T^k , we aim at correcting the period T^k through

$$T^{k+1} = (1 + d\lambda)T^k \approx \sum_{m=0}^Q T_m^{k+1} \psi_m, \quad (3.1)$$

$$T_m^{k+1} = T_m^k + \sum_{i=0}^Q \sum_{j=0}^Q d\lambda_i T_j^k \langle \psi_i \psi_j, \psi_m \rangle, \quad m = 0, \dots, Q, \quad (3.2)$$

where we employed a Galerkin projection using the PC expansion of $d\lambda \in \mathcal{S}^Q$, which is a solution of the minimization problem:

$$\min_{d\lambda \in \mathcal{S}^Q} \|u_I^k - \mathcal{U}(u_I^k, T^k, 1 + d\lambda)\|^2. \quad (3.3)$$

To simplify problem (3.3), we approximate $\mathcal{U}(u_I^k, T^k, 1 + d\lambda)$ by its first order Taylor series representation around $\lambda = 1$, i.e.

$$\mathcal{U}(u_I^k, T^k, 1 + d\lambda) \approx \mathcal{U}(u_I^k, T^k, 1) + \partial_\lambda \mathcal{U}(u_I^k, T^k, 1) d\lambda. \quad (3.4)$$

Inserting (3.4) in (3.3) results in a linearized stochastic optimization problem for the correction term $d\lambda$:

$$\min_{d\lambda \in \mathcal{S}} \|D(u_I^k, T^k, 1) - \partial_\lambda \mathcal{U}(u_I^k, T^k, 1) d\lambda\|^2. \quad (3.5)$$

The corresponding optimality condition reads:

$$2 \left\langle \left(D(u_I^k, T^k, 1) - \partial_\lambda \mathcal{U}(u_I^k, T^k, 1) d\lambda, \partial_\lambda \mathcal{U}(u_I^k, T^k, 1) \right) \right\rangle = 0. \quad (3.6)$$

Introducing the PC expansions of the various stochastic quantities into (3.6) we arrive at the discrete optimality condition for the PC modes $\vec{d}\lambda = [d\lambda_0, \dots, d\lambda_Q]^t \in \mathbb{R}^{Q+1}$:

$$A \vec{d}\lambda = b, \quad (3.7)$$

where $A \in \mathbb{R}^{Q+1, Q+1}$ and $b \in \mathbb{R}^{Q+1}$ are defined by:

$$A_{ml} := \sum_{i,j=0}^P \langle \psi_i \psi_j \psi_l, \psi_m \rangle (\partial_\lambda \mathcal{U}_i^k, \partial_\lambda \mathcal{U}_j^k), \quad b_m := \sum_{i,j=0}^P \langle \psi_i \psi_j, \psi_m \rangle (D_i^k, \partial_\lambda \mathcal{U}_j^k),$$

for $m, l = 0, \dots, Q$. The corresponding Polynomial Chaos coefficients of $\partial_\lambda \mathcal{U}$ and D are given by:

$$\partial_\lambda \mathcal{U}_i^k = \langle \partial_\lambda \mathcal{U}(u_I^k, T^k, 1), \psi_i \rangle, \quad D_i^k = \langle D(u_I^k, T^k, 1), \psi_i \rangle,$$

for $i = 0, \dots, P$.

Lemma 3.1. *The optimization problem (3.5) for $d\lambda = \sum_{i=0}^Q d\lambda_i \psi_i$ is convex.*

Proof. We show that the Hessian of the optimization problem is positive semi-definite. For notational convenience, $\dot{\mathcal{U}}^k$ and D^k are defined by $\dot{\mathcal{U}}^k := \partial_\lambda \mathcal{U}(u_I^k, T^k, 1)$ and $D^k := D(u_I^k, T^k, 1)$. We determine the second partial derivatives of (3.5) with respect to $d\lambda_m$ and $d\lambda_n$, $n, m = 0, \dots, Q$:

$$h_{mn} := \frac{\partial^2}{\partial d\lambda_n \partial d\lambda_m} \|D^k - \dot{\mathcal{U}}^k \sum_{l=0}^Q d\lambda_l \psi_l\|^2 = 2 \langle (\dot{\mathcal{U}}^k \psi_n, \dot{\mathcal{U}}^k \psi_m) \rangle,$$

which defines the Hessian $H := (h_{mn})_{m,n=0}^Q$. Let $y = [y_0, \dots, y_Q]^t \in \mathbb{R}^{Q+1}$, $y \neq 0$ be arbitrary, then the following relations hold:

$$y^t H y = 2 \sum_{m,n=0}^Q y_m \langle (\dot{\mathcal{U}}^k \psi_n, \dot{\mathcal{U}}^k \psi_m) \rangle y_n = 2 \left\| \sum_{m=0}^Q y_m \psi_m \dot{\mathcal{U}}^k \right\|^2 \geq 0.$$

Therefore, H is positive semi-definite, which completes the proof. \blacksquare

Summing up, the determination of the new period update T^{k+1} via (3.1) requires the solution of one or several linear systems of equations, as stated in (3.7), which can be carried out by employing standard direct numerical solvers.

Remark 1. *Note that, because of the linearization error in (3.4), iterations on the period correction can reduce the overall error in (2.21) significantly. For these iterations, after the period has been updated through (3.1), to say T^* , the corresponding terminal state $\mathcal{U}(u_I, T^*, 1)$ is recomputed for the same initial condition u_I^k and used to determine the subsequent correction $d\lambda$. The iterations are stopped whenever $d\lambda$ becomes small enough and finally $T^{k+1} = T^*$.*

3.2. Newton's method for updating the initial condition. Updating the period iterate ensures that the terminal state has a minimal distance with respect to the current initial condition iterate u_I^k . In general the minimum is greater than zero, which necessitates a correction of u_I^k such that the distance can be decreased further.

This is achieved by applying Newton's method to $D(u_I^k, T^{k+1}, 1) = 0$. The corresponding Newton step reads:

$$u_I^{k+1} = u_I^k + du_I^k, \quad -J_k[du_I^k] = D(u_I^k, T^{k+1}, 1), \quad (3.8)$$

where $J_k[du_I^k]$ denotes the Jacobian of $D(u_I, T^{k+1}, 1)$ with respect to u_I in direction du_I^k at $u_I = u_I^k$. Due to the large system size, solving the linear system in (3.8) should be carried out by using iterative solvers, e.g. by the "Generalized Minimal Residual Method" (GMRES method, [23]) suitable for non-symmetric systems. Note that to reduce the computational cost an inexact Newton approach should be used, such that a low accuracy for solving the linear system in (3.8) is sufficient enough to achieve overall convergence, see e.g. [5]. The following section provides a detailed analysis on solving (3.8).

3.3. Solving the Newton step. For each iteration during the solution of (3.8), represented by some iterate w , the "effect" of the Jacobian $J_k[w]$ has to be evaluated. This can be carried out by solving the linearized Navier-Stokes equations, which will be elaborated on in the following.

First we note that the application of the Jacobian J_k to some w can further be simplified by:

$$J_k[w] = w - J_k^{NS}[w],$$

by definition of D , where J_k^{NS} denotes the Jacobian of the terminal state $\mathcal{U}(u_I^k, T^{k+1}, 1)$ in direction w . Therefore, the focus is shifted towards the computation of $J_k^{NS}[w]$, which for the following analysis will be denoted by $J[w]$ for notational convenience. Furthermore, to simplify the derivation of the linear model, divergence free vector spaces for the velocity u arising from the S-SNSE are assumed, such that the pressure variable can be neglected. Also, the strong formulation of the S-SNSE is being considered, provided that the velocity variable fulfils the regularity requirements of a classical solution to the stochastic Navier-Stokes equations. In an analogous yet more technical way, the results of this section can be transferred to the mixed-type variational formulation involving the pressure variable with less regularity requirements on the velocity u .

We define the Navier-Stokes operator F by:

$$F(u_I, u) := \begin{bmatrix} \partial_\lambda u + T(u \cdot \nabla)u - \nu T \Delta u \\ u|_\Gamma - g \\ u(\lambda = 0) - u_I \end{bmatrix},$$

such that $F(u_I, u) = 0$ represents the S-SNSE in their strong formulation subject to a Dirichlet-condition g . Furthermore, let $u_I^* := u_I^k$, then there exists a solution u^* such that $F(u_I^*, u^*) = 0$ [22, 26]. It can be shown that F is C^∞ -differentiable [12] in a neighborhood of (u_I^*, u^*) . The directional Gâteaux derivative of F with respect to u in direction \bar{u} can be easily calculated and reads:

$$F_u(u_I, u)[\bar{u}] = \begin{bmatrix} \partial_\lambda \bar{u} + T(\bar{u} \cdot \nabla)u + T(u \cdot \nabla)\bar{u} - \nu T \Delta \bar{u} \\ \bar{u}|_\Gamma \\ \bar{u}(\lambda = 0) \end{bmatrix}.$$

Assuming that the partial Fréchet derivative F_u is bijective in a neighbourhood of (u_I^*, u^*) allows the use of the implicit function theorem [30] from which it follows:

$$-F_u(u_I, u)u'(u_I) = F_{u_I}(u_I, u), \quad (3.9)$$

for all (u_I, u) in a neighbourhood of (u_I^*, u^*) . Note, that $u'(u_I)[w] = J[w]$ for a direction w . Therefore inserting this relation into equation (3.9) at $(u_I, u) = (u_I^*, u^*)$ with respect to the direction w yields:

$$-\begin{bmatrix} \partial_\lambda v + T(v \cdot \nabla)u^* + T(u^* \cdot \nabla)v - \nu T \Delta v \\ v|_\Gamma \\ v(\lambda = 0) \end{bmatrix} = \begin{bmatrix} 0 \\ 0 \\ -w \end{bmatrix}, \quad (3.10)$$

for $v := J[w]$.

Summing up, the computation of the directional derivative $J[w]$ of the terminal state $\mathcal{U}(u_I^k, T^{k+1}, 1)$ with respect to u_I in direction w does not require a solution of the non-linear form of the S-SNSE. Instead, given an iterate u_I^k and its corresponding terminal state $\mathcal{U}(u_I^k, T^{k+1}, 1)$, it suffices to solve a linearized version of the S-SNSE subject to homogeneous Dirichlet boundary conditions on the boundary $\Gamma \subset \partial\mathcal{D}$ and initial condition w , with linearization around the trajectory of the velocity between the initial condition u_I^k and its terminal state $\mathcal{U}(u_I^k, T^{k+1}, 1)$ as stated in equation (3.10). The weak mixed-type formulation, i.e. with consideration of the pressure variable, results in a non-symmetric system, solution of which can be computed, for example, by applying GMRES as an iterative inner-loop solver again.

Remark 2. *Note, that instead of solving the linearized equations, it is also possible to approximate the Jacobian by a Finite-Difference scheme [4], which, however, would require to solve the non-linear version of the S-SNSE in each iteration.*

3.4. Phase-drift control. Having computed some initial condition iterate u_I^k , it is possible that the trajectories corresponding to different realizations of the random input ξ deviate too much, such that an increasing polynomial degree needs to be employed to capture the stochastic variations. This is due to the arbitrariness of the stochastic phase on the initial

condition definition. Indeed, if $u_I(\xi)$ is a valid initial condition, in the sense that it belongs (a.s.) to the stochastic limit-cycle having a period $T(\xi)$, then $\mathcal{U}(u_I, T(\xi), \beta(\xi))$ is another valid initial condition, $\forall \beta(\xi) > 0$. This can cause numerical instabilities of the algorithm and iterations need to be controlled in an appropriate way. Therefore, we define a control step which ensures that the trajectories remain essentially *in-phase*. This control is based on the ideas initially proposed in [18].

The *phase-drift* can be measured with respect to a deterministic reference trajectory. To this end, we define a reference \hat{u} as the velocity evaluated at the mean $\bar{\xi}$ of the random input, i.e.,

$$\hat{u}(\lambda, x) := u(\lambda, x, \xi)|_{\xi=\bar{\xi}}.$$

The distance between the stochastic velocity field and the reference is defined by

$$\delta u(\lambda, x, \xi) := u(\lambda, x, \xi) - \hat{u}(\lambda, x),$$

such that the *phase-drift* can be measured by the weighted inner product $\Sigma(\lambda, \xi)$ of the distance and the time tangential of the stochastic velocity field:

$$\Sigma(\lambda, \xi) := \frac{(\delta u, \partial_\lambda \hat{u})}{(\partial_\lambda \hat{u}, \partial_\lambda \hat{u})^{1/2}}.$$

Note that $(\partial_\lambda \hat{u}, \partial_\lambda \hat{u}) > 0$ in an almost surely unsteady flow. An *in-phase* condition is equivalent to minimize $\Sigma(\lambda, \xi)$ in some sense, which will be elaborated on in the following. Therefore, in addition to the time scaling by the period T , we introduce a further stochastic time scaling τ , modifying the time scale λ by

$$\tau(t, \xi) := \frac{\lambda(t, \xi)}{\sigma(t, \xi)},$$

where σ is defined to be an almost surely positive random process, which is piecewise constant in the physical time scale t with respect to some finite number of time intervals. Suppose we employ some time discretization scheme of λ , denoted by some function h such that

$$u^{n+1} = u^n + h(\Delta\lambda, u^n, u^{n+1}, \xi),$$

where $u^n := u(\lambda^n)$ and $\Delta\lambda > 0$ denotes a (deterministic) time step size, which can be defined for example by

$$\Delta\lambda := \frac{\Delta t}{T(\bar{\xi})} > 0,$$

for $\Delta t > 0$. Introducing the new stochastic time scaling σ , we get

$$u^{n+1} = u^n + \sigma(\xi)h(\Delta\lambda, u^n, u^{n+1}, \xi),$$

due to σ being piecewise constant in t . Therefore, we obtain the possibility of modifying each time stepping for every trajectory resulting from a realization of ξ . The remaining question is how to define the time scaling σ . Note that $\sigma := 1$ corresponds to no additional time scaling but λ .

In this work we employ a simple heuristic to control the behaviour of σ within each time interval. For this purpose we monitor the quantity $\Sigma(\lambda, \xi)$ and define the "rule":

$$\begin{aligned}\sigma(\xi) &< 1, & \text{if } \Sigma > 0, & \text{ (slow down),} \\ \sigma(\xi) &> 1, & \text{if } \Sigma < 0, & \text{ (speed up).}\end{aligned}$$

Therefore, a trajectory is speeded up, if the angle between the reference and the trajectory is greater than $\pi/2$ and it is slowed down in the other case. As a simple heuristic we define

$$\sigma(\xi) := \left(1 + \theta \frac{1}{\Delta\lambda} (\partial_\lambda u, \partial_\lambda u) \Sigma(\lambda, \xi)\right),$$

where $\theta > 0$ is some prescribed control parameter. Note that this heuristic does not necessary guarantee an almost surely positive σ . However, for a sufficiently small θ it can be assumed that σ remains close to 1, which however reduces the control influence of σ . Furthermore, if the trajectories are *in-phase* σ returns to 1 by definition.

The application of the control step is carried out with respect to one cycle subject to the current period iterate T^k . This requires the solution of the time scaled Navier-Stokes equations, where after completion of one cycle, we choose the velocity with a minimal Σ along the computed trajectory as a new initial condition u_γ^k . In our numerical applications, we chose θ to be the current norm of the distance between the initial condition iterate and its corresponding terminal condition (cf. (2.21)). A small distance suggests that the trajectories should be at least close to *in-phase*, such that no additional phase correction should be necessary.

Remark 3. Note that if θ is chosen too large, then the control becomes numerically unstable, since the positivity constraint could be violated.

3.5. The algorithm. This section shortly recapitulates the algorithm introduced in the previous sections. As can be seen from Algorithm 1, the computation of a periodic orbit requires the solution of various Navier-Stokes problems in each iteration, which is certainly the bulk of the numerical cost. One iteration requires the solution of multiple non-linear stochastic Navier-Stokes problems and multiple linearized stochastic Navier-Stokes problems. Therefore, the numerical efficiency of this algorithm strongly depends on the numerical efficiency on the available numerical solvers for the stochastic Navier-Stokes equations. Especially, in context of high Reynolds number flows, a numerically stable Finite-Element discretization along with the stochastic Galerkin projection requires a large number of degrees of freedom to capture all dynamics of the flow.

Note the the parameter $\gamma > 0$ allows a user control on the accuracy of the computed period iterate, which effects the convergence speed of the algorithm. In our computations shown in section 4 it was sufficient to choose $\gamma = 1.0$.

4. Numerical results. The algorithm described in the previous section shall be verified employing a slightly modified benchmark problem originally introduced in [25]. It is a two-dimensional problem in the spatial variable, which describes a flow of an incompressible fluid around a circular domain within a channel of length L and height H . Its exact geometrical data as well as the employed Finite-Element mesh consisting of triangles is depicted in Fig. 4.1

Algorithm 1 Computation of stochastic periodic orbits

- 1: Choose initial guesses u_I^0 and T^0
- 2: Choose tolerances $\epsilon > 0$, $\gamma > 0$ and $k_{max} \in \mathbb{N}$
- 3: $k \leftarrow 0$
- 4: Compute terminal condition $u_T^0 \leftarrow \mathcal{U}(u_I^0, T^0, 1)$ (non-linear stochastic NS)
- 5: $r^0 \leftarrow \|u_I^0 - u_T^0\| / \|u_I^0\|$
- 6: **while** $k < k_{max}$ **and** $r^k > \epsilon$ **do**
- 7: $k \leftarrow k + 1$
- 8: Correct initial condition u_I^{k-1} by phase control (non-linear stochastic NS)
- 9: **while** $\|d\lambda\| > \gamma \|r^{k-1}\|$ **do**
- 10: Compute $d\lambda = \sum_{i=0}^M d\lambda_i \psi_i$ (non-linear stochastic NS)
- 11: Update period modes $T_m^k \leftarrow T_m^{k-1} + \sum_{i=0}^M \sum_{j=0}^Q d\lambda_i T_j^{k-1} \langle \psi_i \psi_j, \psi_m \rangle$, $m = 0, \dots, Q$
- 12: **end while**
- 13: Compute terminal condition $u_T^k \leftarrow \mathcal{U}(u_I^{k-1}, T^k, 1)$ (non-linear stochastic NS)
- 14: Solve inexact Newton step $-J_k[du_I^k] = u_I^{k-1} - u_T^k$ (linear stoch. NS, multiple times)
- 15: Update initial condition $u_I^k \leftarrow u_I^{k-1} + du_I^k$
- 16: Compute terminal condition $u_T^k \leftarrow \mathcal{U}(u_I^k, T^k, 1)$ (non-linear stochastic NS)
- 17: $r^k \leftarrow \|u_I^k - u_T^k\| / \|u_I^k\|$
- 18: **end while**
- 19: Postprocessing

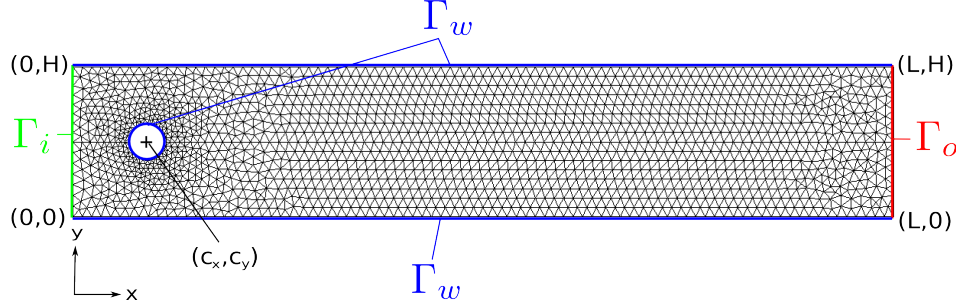


Figure 4.1: Employed geometry and triangulation of a 2d-channel with a circular domain.

with $L = 2.2$, $H = 0.4$. The circular domain has a diameter of $D_c = 0.1$ and its center-point has the coordinates $(c_x, c_y) = (0.2, 0.2)$.

No-slip boundary conditions are considered for $\Gamma_w \subset \partial\mathcal{D} = (0, L) \times (0, H)$. The inflow boundary condition at $\Gamma_i \subset \partial\mathcal{D}$ is set to be a stochastic parabolic profile, i.e.,

$$u_x(0, y, t; \xi) = 4v^{(1)}(\xi)y(H-y)/H^2 + v^{(2)}(\xi) \sin(2\pi y/H), \quad y \in [0, H], \quad t \geq 0, \quad (4.1)$$

$$u_y(0, y, t; \xi) = 0, \quad t \geq 0, \quad (4.2)$$

with $u = [u_x, u_y]$ denoting the components in x- and y-directions of the velocity u , respectively.

In the following sections, a one-dimensional and a two-dimensional uniformly distributed random input ξ will be considered, where $v^{(1)}(\xi)$ and $v^{(2)}(\xi)$ will be defined later according to the numerical examples. For the outflow boundary condition at $\Gamma_o \subset \partial\mathcal{D}$ so-called "do-nothing" boundary conditions are applied [11]. These represent natural boundary conditions arising from the weak formulation of the SNSE by requiring all boundary integrals at Γ_o to vanish in their sum, i.e.,

$$\int_{\Gamma_o} \nabla u_i \cdot \vec{n} - p_i \vec{n} \, dx = 0, \quad i = 0, \dots, P,$$

where u_i and p_i , $i = 0, \dots, P$ denote the PC modes of the velocity and pressure variable, respectively and \vec{n} denotes the outward unit normal vector on the boundary Γ_o . Since this boundary condition results in a unique pressure variable, no additional requirements, such as $\int_{\mathcal{D}} p \, dx = 0$, are necessary.

For time integration a Crank-Nicolson scheme with a homogeneous time step size $\Delta t = 0.01$ for the unscaled time variable t is employed. The corresponding time step length $\Delta\lambda > 0$ for the scaled time variable λ is defined by:

$$\Delta\lambda := \frac{\Delta t}{T^k(\xi = \bar{\xi})},$$

Therefore, the time step size can vary for each iteration k of the algorithm, depending on the value $T^k(\bar{\xi})$ of the period iterate. The spatial variable is discretized employing the Finite-Element mesh depicted in Fig. 4.1 and stable Taylor-Hood elements of order 2 for each stochastic mode of the velocity variable and order 1 for each pressure mode. The computations are carried out using the Finite-Element software *HiFlow*³ [1].

Furthermore, the kinematic viscosity ν is deterministic and set to $\nu = 0.001$ for all benchmark computations. The Reynolds number is calculated by:

$$Re(\xi) = \frac{2}{3} \frac{v^{(1)}(\xi) D_c}{\nu}.$$

In the following numerical examples, we choose $v^{(1)}$ and $v^{(2)}$ such that a laminar time-periodic solution exists, which does not require any additional stabilization of the convective term. The flow is characterized by a periodic vortex shedding scheme behind the circular domain (the flow is considered from left to right, cf. Fig. 4.1).

4.1. One-dimensional random input. In this section a one-dimensional random input $\xi \sim U(-1, 1)$, uniformly distributed in the interval $(-1, 1)$, is being considered. The random quantities $v^{(1)}(\xi)$ and $v^{(2)}(\xi)$ for the inflow boundary conditions (4.1) are set to:

$$v^{(1)}(\xi) := 1.5 + 0.15\xi, \quad v^{(2)}(\xi) := 0,$$

representing a stochastic parabolic inflow condition, which results in a uniformly distributed Reynolds number $Re \sim U(90, 110)$. Note that the uncertainty in the Reynolds number is introduced by the stochastic inflow condition only, since a deterministic viscosity $\nu = 0.001$ is used throughout the numerical computations.

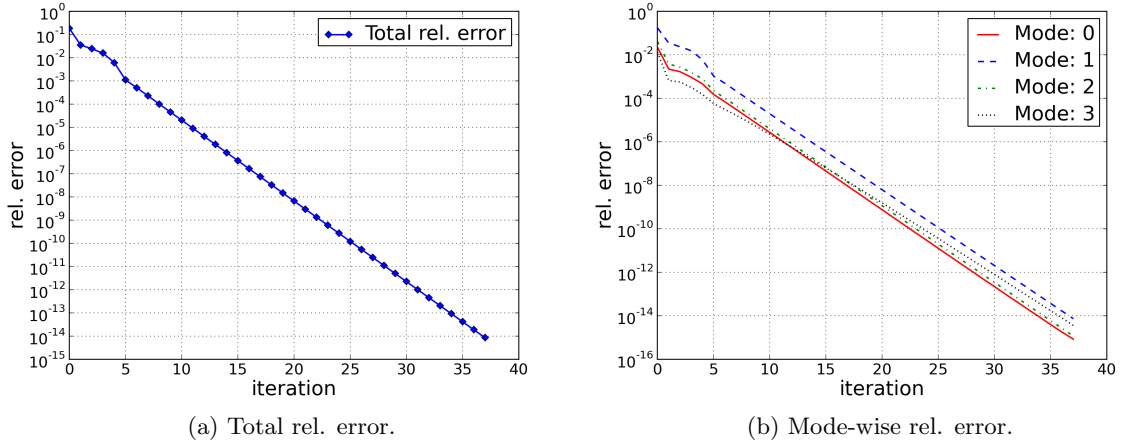


Figure 4.2: Total and mode-wise relative error developments with respect to the number of iterations for a third order PC expansion.

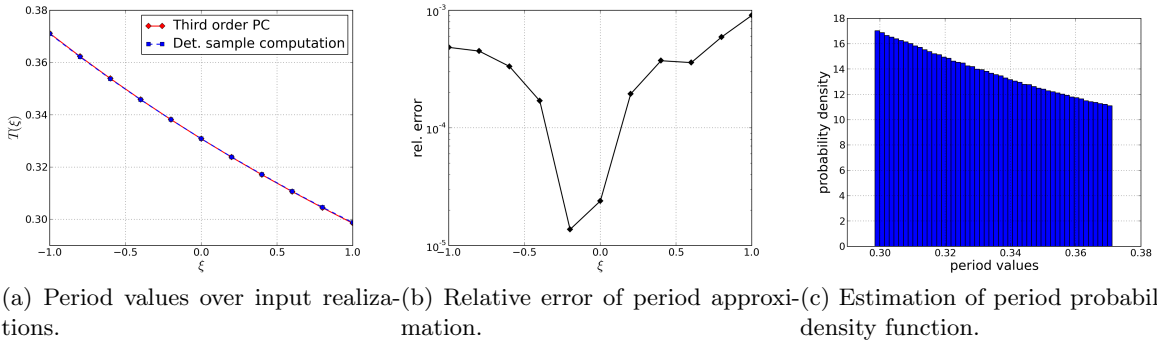


Figure 4.3: Period approximation and pdf estimation with absolute values and relative errors compared to deterministic simulations. A deterministic sample value corresponds to the period value computed by applying the algorithm on a deterministic system obtained by specific realizations of the random input ξ at the plotted nodes. The "Third order PC" labelled period corresponds to the point evaluation of the PC expansion of the stochastic period.

We use a fully developed deterministic flow with corresponding deterministic period as an initial guess for the iteration procedure. For verification of the convergence properties of the algorithm we consider the relative errors based on the difference of the initial condition and its terminal state with respect to each iteration. Thereby, the total as well as the mode-wise

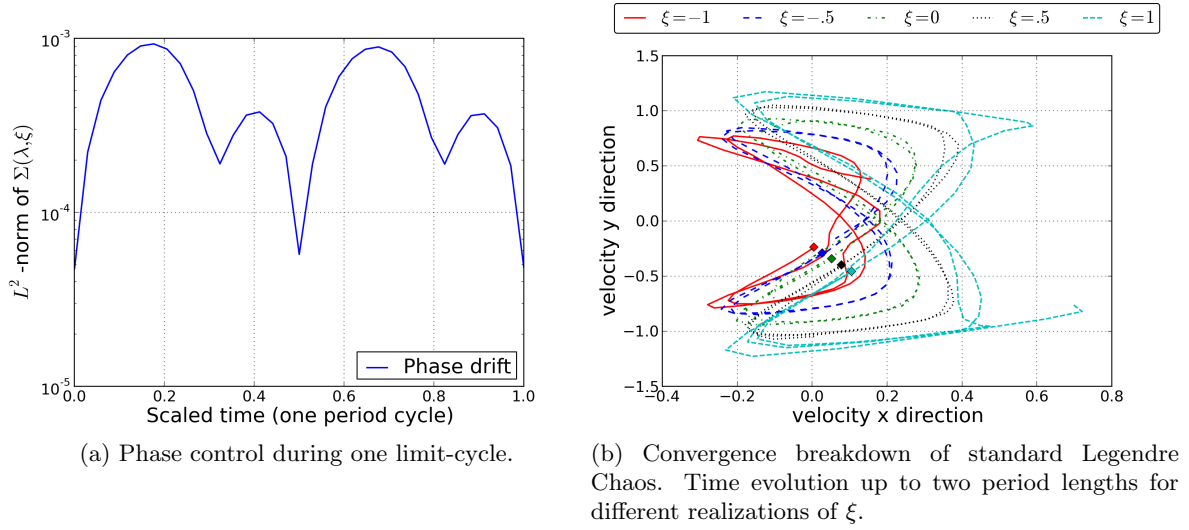
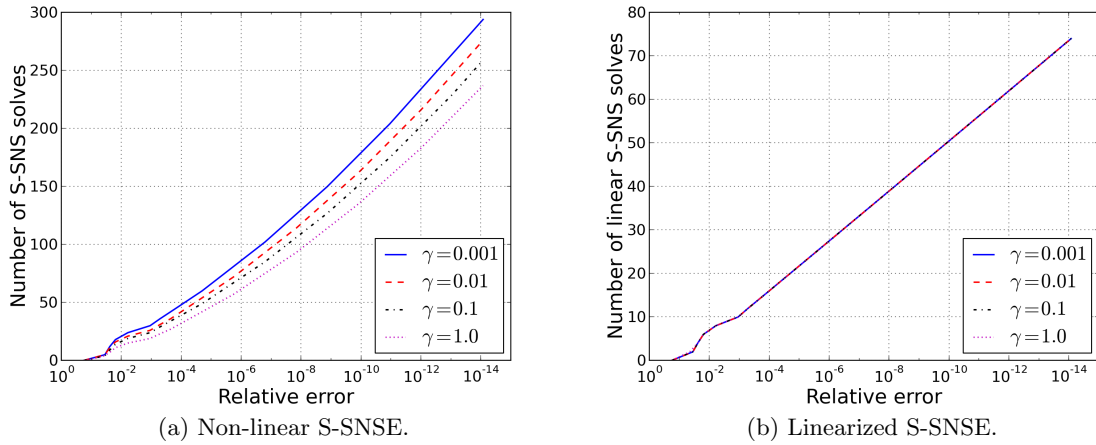


Figure 4.4: Phase control and convergence breakdown of standard third order Legendre Chaos.

Figure 4.5: Required number of solves of the linearized and non-linear S-SNSE with respect to desired accuracy and control parameter γ .

relative errors are computed by the following relations:

$$\epsilon := \frac{\|u(\lambda = 1) - u(\lambda = 0)\|_{W \otimes \mathcal{S}^P}}{\|u^{final\ iteration}\|_{L^2((0,T) \times \mathcal{D} \times \Omega)}}, \quad \epsilon^i := \frac{\|u_i(\lambda = 1) - u_i(\lambda = 0)\|_W}{\|u^{final\ iteration}\|_{L^2((0,T) \times \mathcal{D} \times \Omega)}}$$

The computations are carried out employing a 3^{rd} order Legendre PC expansion resulting in $P + 1 = 4$ modes. As can be observed in Fig. 4.2 the total as well as mode-wise relative

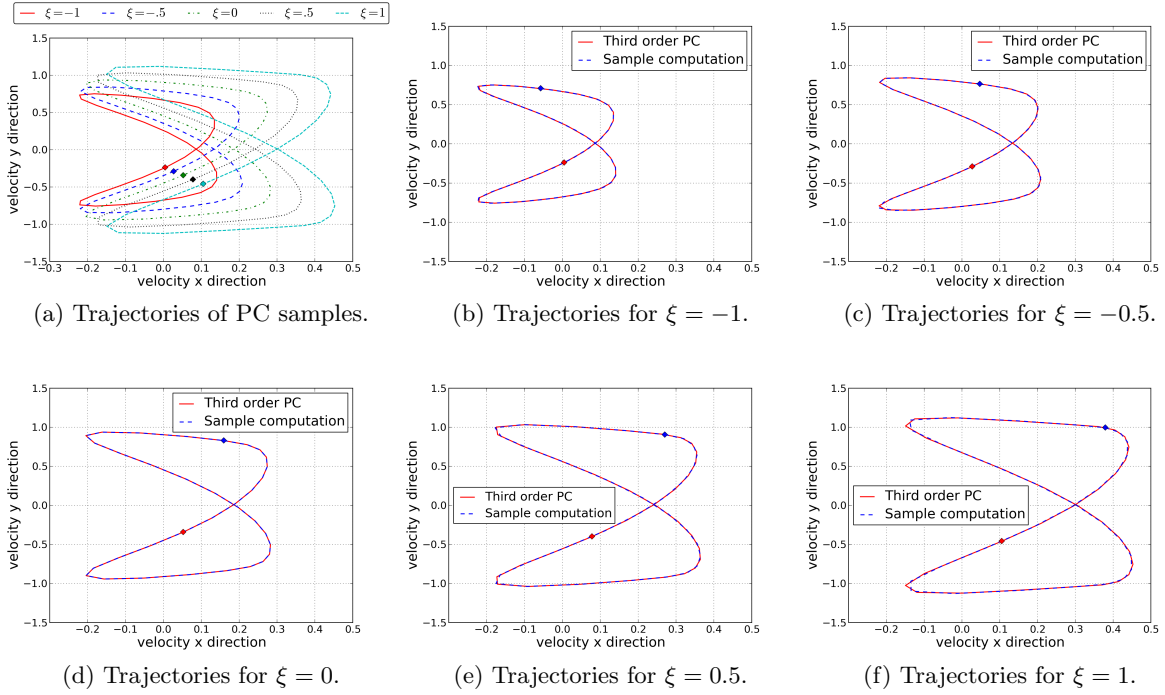


Figure 4.6: Limit-cycles for PC solution and corresponding sample computations based on the solution of the deterministic reference systems obtained by a realization of the random input ξ .

errors decrease exponentially with respect to the number of iterations starting at the initial errors introduced by the initial guess up to machine precision. Furthermore, Fig. 4.3a and 4.3b depict the absolute values and corresponding relative errors associated with the point-wise evaluation of the period computed by the PC expansion and corresponding deterministic sample computations. It can be observed that the period samples are approximated with an accuracy up to the order $O(10^{-3})$. We stress that the relation of the period $T(\xi)$ and ξ is nonlinear, which is verified by estimating the probability density function of $T(\xi)$ (cf. Fig 4.3c). Fig. 4.4a depicts the evolution of the *phase-drift*, measured by $\|\Sigma(\lambda, \xi)\|_S$ (cf. Section 3.4), during one cycle. It can be observed, that the phase control keeps the trajectories in phase (in a L^2 sense), which stabilizes the numerical computation and allows for lower order PC expansions. Furthermore, we observe that the phase control exhibits a period with about twice the length of the period of the flow, which is due to the symmetry of the trajectories.

Fig. 4.4b depicts a standard third order Legendre PC expansion computed by a straight forward time integration without employing the introduced algorithm. The standard approach leaves the limit cycle after a very short time and is not able to complete even one cycle. This can be explained by an increasing *phase-drift* in the trajectories, which requires an increasing polynomial degree in time. Note, that the introduced algorithm also employs a Legendre PC expansion due to the Uniform distribution of the random input.

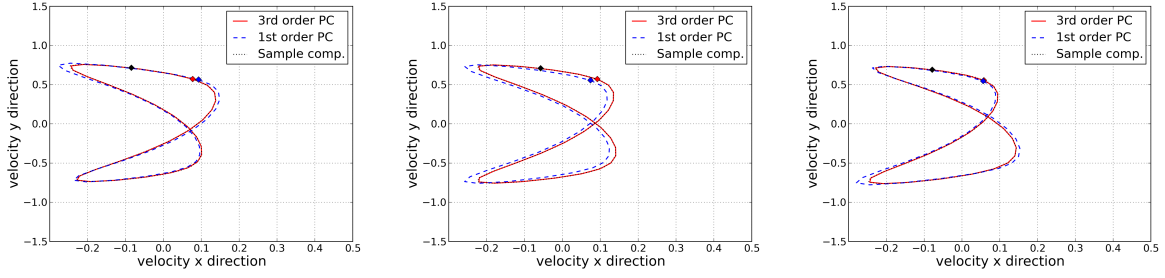
Although the decrease of the relative errors in Fig. 4.2 suggest a high accuracy in computing the almost surely time-periodic limit-cycles of the trajectories, we verify the limit-cycles by a comparison of the stochastic PC approach and a purely deterministic reference simulation employing the same algorithm. The trajectories are depicted in Fig. 4.6. It can be observed that the dependence on ξ has a significant impact on the shape and magnitude of the limit-cycles. Furthermore, there is a good agreement between the deterministic computations and the point evaluation of the PC solutions. In addition, the initial condition realizations at time $\lambda = 0$ are marked in the plots. Since the computations are carried out using an implicit time discretization scheme, the numerical stability allows for a large time step size resulting in time steps varying between 30 and 38. Fig. 4.5 depicts the required number of solves of the non-linear S-SNSE as well as its linearized counterpart to achieve a certain relative error, where the value $\gamma = 1.0$ results in the least number of required solves. Achieving machine precision requires about 230 non-linear and 75 linearized solves, in contrast, e.g. the solution up to the relative error of 10^{-4} requires about 30 non-linear and 15 linearized solves. We stress that the numerical cost of the algorithm is proportional to the number of required S-SNSE solves. Overall, the numerical algorithm is capable of computing the stochastic limit-cycles with a high accuracy and overcomes the convergence breakdown of a standard PC expansion.

4.2. Two-dimensional random input. In this section the algorithm shall be applied to a more complex problem, characterized by a two-dimensional random input $\xi = (\xi_1, \xi_2)$, where $\xi_1, \xi_2 \sim U(-1, 1)$, i.e. we consider a two-dimensional independent uniformly distributed random vector in the interval $(-1, 1)$. The random quantities $v^{(1)}(\xi)$ and $v^{(2)}(\xi)$ for the inflow boundary conditions (4.1) are set to:

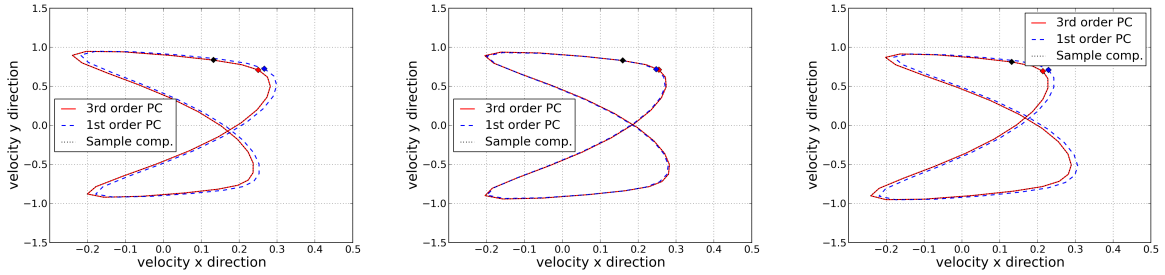
$$v^{(1)}(\xi) := 1.5 + 0.15\xi_1, \quad v^{(2)}(\xi) := 0.15\xi_2,$$

representing a stochastic parabolic inflow condition, with respect to ξ_1 and a stochastic sinus profile with respect to ξ_2 . It is ensured that the inflow boundary condition remains positive almost surely.

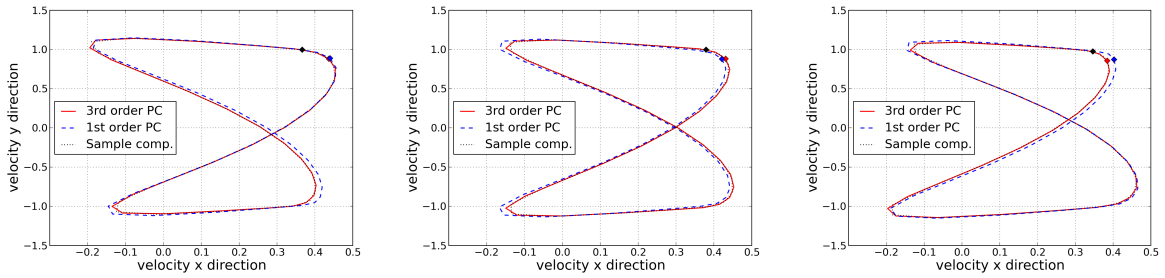
The numerical computations are carried out up to a total relative error of order $O(10^{-9})$. We have observed that the period exhibits a dominant one-dimensional dependence on ξ_1 . There is only a small dependence of the period on ξ_2 (not pictured). Therefore, the probability density exhibits a similar behaviour as for the one-dimensional random input case (cf. Fig. 4.3c). Although ξ_2 has little effect on the period $T(\xi_1, \xi_2)$, the corresponding limit-cycles exhibit a significant dependence on both ξ_1 and ξ_2 . This is verified by a comparison of deterministic reference scenarios and corresponding realizations of a third order Legendre PC solution in Fig. 4.7. Furthermore, the results are compared to a first order Legendre PC expansion to demonstrate the dependence of the limit-cycle approximation on the order of the PC expansion. It can be observed, that the third order expansion is capable of approximating each deterministic reference solution with high accuracy. In contrast, the first order expansion exhibits a significant deviation to the deterministic reference scenarios. However, this demonstrates the convergence with respect to the order of the PC expansion and stresses the importance of verifying the PC solutions according to their sample realizations. Fig. 4.8 provides a summary of the different third order PC realizations to give a compact view on the dependence of the limit-cycles on the random input ξ_1 and ξ_2 .



(a) Trajectories for $\xi_1 = -1, \xi_2 = -1$. (b) Trajectories for $\xi_1 = -1, \xi_2 = 0$. (c) Trajectories for $\xi_1 = -1, \xi_2 = 1$.



(d) Trajectories for $\xi_1 = 0, \xi_2 = -1$. (e) Trajectories for $\xi_1 = 0, \xi_2 = 0$. (f) Trajectories for $\xi_1 = 0, \xi_2 = 1$.



(g) Trajectories for $\xi_1 = 1, \xi_2 = -1$. (h) Trajectories for $\xi_1 = 1, \xi_2 = 0$. (i) Trajectories for $\xi_1 = 1, \xi_2 = 1$.

Figure 4.7: Limit-cycles for PC solution and corresponding sample computations based on the solution of the deterministic reference systems obtained by a realization of the random input $\xi = (\xi_1, \xi_2)$.

5. Conclusions. This paper is focused on the application of Polynomial Chaos (PC) to fluid flow problems exhibiting stochastic limit-cycles, i.e., almost surely time-periodic solutions with uncertain period. A standard PC expansion is known to break down in convergence for this kind of problems because of strong non-linear dynamics. This necessitates the development of appropriate numerical solvers overcoming the restrictions given by fixing a polynomial degree of an PC expansion. In this work, we introduce a numerical algorithm based on a reformulation of the governing equations by introducing the period as an unknown stochastic random variable to the unsteady incompressible Navier-Stokes equations subject to random

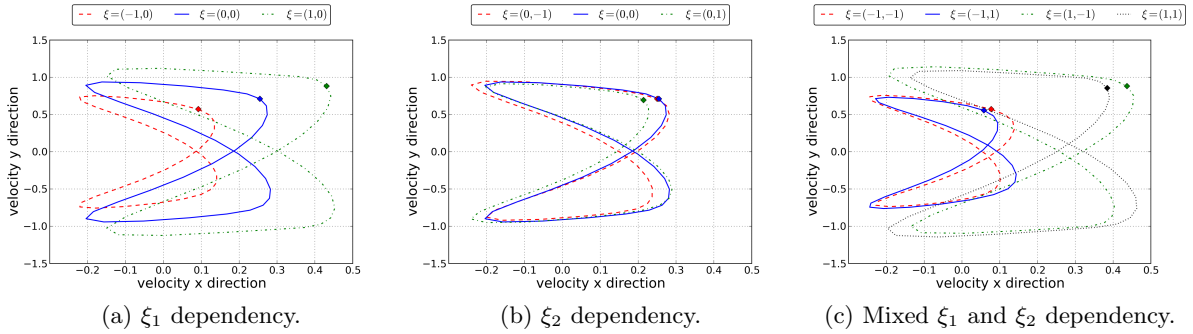


Figure 4.8: Point evaluation of limit-cycles of the 3rd order PC solution.

input. This additional random variable is computed by an optimality constraint, which corrects the error associated with the stochastic realizations of the period. Since a time-periodic solution can be characterized by a period and some corresponding initial condition of the flow at time $t = 0$, a Newton-step is applied to provide an update formula for computing a new iterate of the initial condition. However, this doesn't ensure automatically that the trajectories corresponding to the realizations of the stochastic flow remain *in-phase* when integrating the governing equations in time. This can result in an increasing demand on the PC order to accurately approximate the initial condition. But since the initial condition is not unique, there exists another representative which requires a much lower expansion order, characterized by *in-phase* trajectories. Therefore, a stabilization step based on an heuristic optimization technique is introduced, which ensures that the trajectories remain *in-phase* when integrating in time.

The algorithm is applied to a benchmark problem representing a flow around a circular domain subject to a one- and a two-dimensional random input at the inflow boundary condition. For both cases excellent convergence results are achieved by employing a third order PC expansion. The algorithm itself exhibits an exponential convergence rate. Furthermore, the limit-cycles and the period are in very good agreement to deterministic reference solutions. However, one must pay attention to the employed order of the PC expansion. If a low PC expansion order is used, the solutions also follow a stochastic limit-cycle, but the trajectories are unable to capture the dynamics of the deterministic reference scenario, which requires an increase in the PC expansion order.

The numerical cost of the algorithm strongly depends on the employed numerical solvers for the solution of the stochastic Navier-Stokes equations, since these need to be solved multiple times during one iteration. Machine precision for the first benchmark problem was obtained by the solution of about 230 non-linear S-SNSE and 75 linearized S-SNSE solves. The growth of the computational cost is exponential with respect to the achieved relative error. This is due to the linearization error arising from computing the period update, whose reduction results in a growing number of S-SNSE solves with respect to a prescribed relative error.

Statistical properties of the random parameters, such as for example their mean, their variance or their probability distribution, could theoretically have an effect on the convergence

rate of the algorithm. A large stochastic variation in the period, for example, could result in more correction steps necessary for determining the period update. Future publications will provide a detailed quantitative analysis on the dependence of the convergence and associated numerical cost of the algorithm with respect to the statistical properties.

REFERENCES

- [1] H. ANZT, W. AUGUSTIN, M. BAUMANN, T. GENGENBACH, T. HAHN, A. HELFRICH-SCHKARBANENKO, V. HEUVELINE, E. KETELAER, D. LUKARSKI, A. NESTLER, S. RITTERBUSCH, S. RONNAS, M. SCHICK, M. SCHMIDTOBREICK, C. SUBRAMANIAN, J.-P. WEISS, F. WILHELM, AND M. WLOTZKA, *Hiflow3: A hardware-aware parallel finite element package*, in Tools for High Performance Computing 2011, Holger Brunst, Matthias S. Müller, Wolfgang E. Nagel, and Michael M. Resch, eds., Springer Berlin Heidelberg, 2012, pp. 139–151.
- [2] P.S. BERAN, C.L. PETTIT, AND D.R. MILLMAN, *Uncertainty quantification of limit-cycle oscillations*, *J. Comput. Phys.*, 217 (2006), pp. 217–247.
- [3] B.M. BOGHOSIAN, L.M. FAZENDEIRO, J. LÄTT, H. TANG, AND P.V. COVENEY, *New variational principles for locating periodic orbits of differential equations*, *Philos. Transact. A, Math. Phys. Eng. Sci.*, 369 (2011), pp. 2211–2218.
- [4] YOHANN DUGUET, CHRIS C. T. PRINGLE, AND RICH R. KERSWELL, *Relative periodic orbits in transitional pipe flow*, *Physics of fluids*, 20 (2008).
- [5] STANLEY C. EISENSTAT AND HOMER F. WALKER, *Choosing the forcing terms in an inexact newton method*, *SIAM J. Sci. Comput.*, 17 (1994), pp. 16–32.
- [6] C. A. J. FLETCHER, *Computational Techniques for Fluid Dynamics, Vol I and II*, Computational Physics, Springer, 1988.
- [7] MARC GERRITSMAN, JAN-BART VAN DER STEEN, PETER VOS, AND GEORGE EM KARNIADAKIS, *Time-dependent generalized polynomial chaos*, *Journal of Computational Physics*, 229 (2010), pp. 8333–8363.
- [8] ROGER GHANEM AND P. D. SPANOS, *Stochastic finite elements: A spectral approach*, Springer-Verlag New York, NY, 1991.
- [9] J.-L. GUERMOND, P. MINEV, AND J. SHEN, *An overview of projection methods for incompressible flows*, *Computer Methods in Applied Mechanics and Engineering*, 195 (2006), pp. 6011–6045.
- [10] VINCENT HEUVELINE AND MICHAEL SCHICK, *A hybrid generalized Polynomial Chaos method for stochastic dynamical systems*, *International Journal for Uncertainty Quantification*, to appear (2014).
- [11] JOHN G. HEYWOOD, ROLF RANNACHER, AND STEFAN TUREK, *Artificial boundaries and flux and pressure conditions for the incompressible navier-stokes equations*, tech. report, 1992.
- [12] MICHAEL HINZE, RENE PINNAU, MICHAEL ULBRICH, AND STEFAN ULBRICH, *Optimization with PDE Constraints*, vol. 23 of Mathematical Modelling: Theory and Applications, Springer Science + Business Media B.V., 2009.
- [13] O.M. KNIO AND O.P. LE MAÎTRE, *Uncertainty propagation in CFD using polynomial chaos decomposition*, *Fluid Dyn. Res.*, 38 (2006), pp. 616–640.
- [14] O.P. LE MAÎTRE, O.M. KNIO, H.N. NAJM, AND R.G. GHANEM, *A stochastic projection method for fluid flow. I. Basic formulation*, *J. Comput. Physics*, 173 (2001), pp. 481–511.
- [15] ———, *Uncertainty propagation using Wiener-Haar expansions*, *J. Comput. Physics*, 197 (2004), pp. 28–57.
- [16] O.P. LE MAÎTRE, M.T. REAGAN, H.N. NAJM, R.G. GHANEM, AND O.M. KNIO, *A stochastic projection method for fluid flow. II. Random process*, *J. Comput. Physics*, 181 (2002), pp. 9–44.
- [17] OLIVIER P. LE MAÎTRE AND OMAR M. KNIO, *Spectral Methods for Uncertainty Quantification : With Applications to Computational Fluid Dynamics*, Springer Science+Business Media B.V, Dordrecht, 2010.
- [18] OLIVER P. LE MAÎTRE, LIONEL MATHELIN, OMAR M. KNIO, AND M. YOUSUFF HUSSAINI, *Asynchronous time integration for polynomial chaos expansion of uncertain periodic dynamics*, *Discrete and Continuous Dynamical Systems*, 28 (2010), pp. 199–226.
- [19] OLIVIER P. LE MAÎTRE, H.N. NAJM, R.G. GHANEM, AND O.M. KNIO, *Multi-resolution analysis of Wiener-type uncertainty propagation schemes*, *Journal of Computational Physics*, 197 (2004), pp. 502

– 531.

- [20] CATHERINE E. POWELL AND DAVID J. SILVESTER, *Preconditioning steady-state navier–stokes equations with random data*, SIAM Journal Sci. Comp., 34 (2012), pp. 2482–2506.
- [21] CATHERINE E. POWELL AND ELISABETH ULLMANN, *Preconditioning stochastic galerkin saddle point systems*, SIAM J. Matrix Anal. & Appl., 31 (2010), pp. 2813–2840.
- [22] ALFIO QUARTERONI AND ALBERTO VALLI, *Numerical approximation of partial differential equations*, Springer series in computational mathematics, Springer, Berlin, 1994.
- [23] YOUSEF SAAD AND MARTIN H. SCHULTZ, *GMRES: A generalized minimal residual algorithm for solving nonsymmetric linear systems*, SIAM J. Sci. Stat. Comput., 7 (1986), pp. 856–869.
- [24] T. P. SAPSIS AND P. F.J. LERMUSIAUX, *Dynamically orthogonal field equations for continuous stochastic dynamical systems*, Physica D, 238 (2009), pp. 2347–2360.
- [25] M. SCHÄFER, S. TUREK, F. DURST, E. KRAUSE, AND R. RANNACHER, *Benchmark computations of laminar flow around a cylinder*, in Flow Simulation with High-Performance Computers II, vol. 48 of Notes on Numerical Fluid Mechanics (NNFM), Springer, 1996, pp. 547–566.
- [26] ROGER TEMAM, *Navier-Stokes equations : theory and numerical analysis*, AMS Chelsea Publ., Providence, RI, reprinted with corr. ed., 2001.
- [27] STEFAN TUREK, *Efficient Solvers for Incompressible Flow Problems: An Algorithmic and Computational Approach*, vol. 6 of Lecture Notes in Computational Science and Engineering, Springer, 1999.
- [28] XIAOLIANG WAN AND GEORGE EM KARNIADAKIS, *Multi-element generalized polynomial chaos for arbitrary probability measures*, SIAM Journal on Scientific Computing, 28 (2006), pp. 901–928.
- [29] NORBERT WIENER, *The homogeneous chaos*, American Journal of Mathematics, 60 (1938), pp. 897–936.
- [30] EBERHARD ZEIDLER, *Applied functional analysis : applications to mathematical physics*, Applied mathematical sciences, Springer, New York, corr. 3. print. ed., 1999.